

RSC Advances



This is an *Accepted Manuscript*, which has been through the Royal Society of Chemistry peer review process and has been accepted for publication.

Accepted Manuscripts are published online shortly after acceptance, before technical editing, formatting and proof reading. Using this free service, authors can make their results available to the community, in citable form, before we publish the edited article. This *Accepted Manuscript* will be replaced by the edited, formatted and paginated article as soon as this is available.

You can find more information about *Accepted Manuscripts* in the [Information for Authors](#).

Please note that technical editing may introduce minor changes to the text and/or graphics, which may alter content. The journal's standard [Terms & Conditions](#) and the [Ethical guidelines](#) still apply. In no event shall the Royal Society of Chemistry be held responsible for any errors or omissions in this *Accepted Manuscript* or any consequences arising from the use of any information it contains.

Porous CoS_2 is synthesized by a modified molten-salt synthesis approach with the specific capacitance as high as 654 F g^{-1} .

Cite this: DOI: 10.1039/c0xx00000x

www.rsc.org/xxxxxx

ARTICLE TYPE

A facile template-free approach for the solid-phase synthesis of CoS₂ nanocrystals and their enhanced storage energy in supercapacitor

Ying Ji, Xiaoyang Liu*, Wei Liu, Ying Wang, Hongdan Zhang, Min Yang, Xiaofeng Wang, Xudong Zhao and Shouhua Feng

Received (in XXX, XXX) Xth XXXXXXXXX 20XX, Accepted Xth XXXXXXXXX 20XX
DOI: 10.1039/b000000x

Sphere-like CoS₂ nanocrystals (NCs) with porous surfaces were prepared by a modified molten-salt synthesis (MSS) method under mild reaction conditions. Thiourea was used as a reactant, flux and structure-directing agent in the synthesis of CoS₂ NCs, which led to mild reaction conditions, pure product and porous sphere surface. The increase of reaction temperature and molar ratio of cobalt nitrate to thiourea results in larger CoS₂ NCs and the change of their morphologies from spheroidal to angular. The synthesis mechanism of CoS₂ nanocrystals includes three steps which are the formation of sphere-like CoS₂ NCs at the early reaction stage, the formation of porous structure on the CoS₂ NC surface and the aggregation of NCs. The specific surface area of CoS₂ NCs electrode reached 29.30 m²g⁻¹ which results in a specific capacitance as high as 654 F.g⁻¹. These results demonstrate that CoS₂ NCs can be produced in large scale through a simple solid-phase synthesis pathway and it will be a promising electrode material for supercapacitors.

1. Introduction

The increasing demand for energy and environmental protection has stimulated intensive research into energy storage and conversion from alternative energy sources.¹⁻³ Supercapacitor is one of most promising energy storage techniques due to its high energy and power density, long cycling life and safe operation.⁴⁻⁶ A long-standing supercapacitor hypothesis is that large specific surface area (SSA) can efficiently induce the electrolyte ions to contact the active sites for Faradaic energy storage.⁷⁻⁹ Therefore, efforts have been made to improve the morphologies and structures of electrode materials for supercapacitor. Porous structure provides high surface area of a solid material, facilitates diffusion of foreign substances throughout the bulk, and thus improves its performance in various applications.^{10,11} The porous materials have also been used as electrodes for various supercapacitors.¹²⁻¹⁵

Cobalt sulfide has a variety of oxidation states for charge transfer, which makes it an excellent electrode material in supercapacitors. It has been reported that cobalt sulfides nanocrystals (NCs) show electrochemical stability, excellent capacitive properties and relatively good cycle stability in supercapacitor and lithium-ion batteries.¹⁶⁻²² In addition, cobalt sulfides have also been widely used in many other industries.²³⁻²⁷ However, the synthesis of CoS₂ NCs has not been well established.^{15,28} Its preparation by conventional solid-state synthesis process requires organic surfactants, high reaction temperature, inert gas and complex operation.²⁹ Molten-salt method (MSS) has been reported for the synthesis of cobalt sulfides.³⁰⁻³² However, sulfides are unstable at high temperature

and are converted to sulfur dioxide at temperatures of 300 °C and higher. Thus, an atmosphere of inert gas is needed to protect the synthesized sulfides from the degradation, which limits the application of the MSS method.

In the present work, we proposed a facile template-free MSS method for large-scale synthesis of sphere-like CoS₂ NCs with porous surface for the first time. Cobalt nitrate and thiourea were used as reactants. Thiourea was also used as the flux to replace the toxic and expensive salts in the conventional synthesis process.³³ The reaction temperature was reduced to 180 °C due to the low melting point of thiourea, which provides a stable environment for the synthesized sulfides. In addition, no other impurity ions were introduced in the reactor, which results in high purity products. The effects of reaction time and the ratio of the reactants on the size and morphology of CoS₂ NCs were explored. The synthesized CoS₂ NCs through this modified MSS method showed high specific capacitance for pseudocapacitor.

2. Experimental section

2.1 Materials

Cobalt nitrate (Co(NO₃)₂·6H₂O, 99.99 %) was purchased from Tianjin Chemical Reagent Ltd (Tianjing, China). Nickle foam was purchased from Kunshan Dessco Electron Co., Ltd (Kunshan, China). Thiourea (99.0%), analytical grade potassium hydroxide (KOH, 96.0%) and ethanol were purchased from Beijing Chemical Reagent Ltd (Beijing, China). Acetylene black (99.5%) was purchased from Alfa Aesar (Ward Hill, MA). All reagents were used without further purification.

2.2 Molten-salt synthesis of CoS₂ NCs

Cobalt nitrate and thiourea were mixed at a molar ratio of 1:5 in a crucible and heated at 180 °C for 4 h unless stated otherwise. The amount of cobalt nitrate added resulted in 1.0 mmol Co in the product. The product was allowed to cool to room temperature, washed with deionized water and ethanol several times, and dried at 60 °C.

2.3 Characterizations of CoS₂ NCs

The phase purity of the CoS₂ NCs was examined by X-ray powder diffraction (XRD) on a Rigaku D/max 2550VB diffractometer at a scanning rate of 10 °/min in the 2θ range from 10 to 80°. The morphology and size of the as-synthesized products were determined with a scanning electron microscopy (SEM, JSM-6700F, JEOL, Japan) and a transmission electron microscopy (TEM, Hitachi H-800 electron microscope) equipped with a CCD camera at an accelerating voltage of 200 kV. High-resolution TEM (HRTEM) images were collected on a JEM-2100F electron microscope. The elementary analysis was performed on a VG ESCALAB MKII X-ray photoelectron spectroscopy (XPS) equipped with a Mg Kα excitation (1253.6 eV) source. The binding energy was calibrated with C 1s at 284.6 eV. The Brunauer-Emmett-Teller (BET) surface area of the CoS₂ NCs was measured with N₂ adsorption at 77 K on an ASAP 2420 Micromeritic system (Micromeritic, Japan). Infrared spectra of the samples were recorded by Perkin-Elmer IR spectrometer using a KBr pellet.

3. Results and discussion

3.1. Synthesis and characterizations of CoS₂ NCs

SEM image of the synthesized CoS₂ NCs shows that they are ~150 nm spheroids with porous surface (Fig. 1a). Ultra-small particles are found in the spheroids as shown in their TEM image (Fig. 1b). It illustrates that the CoS₂ NCs are aggregated by smaller monomers, forming this porous structure. Lattice fringes with spacings of 0.23 nm and 0.40 nm were observed in the high-resolution TEM (HRTEM) image of CoS₂ spheroids, which are attributed to the (211)-facet and (110)-facet *d*-spacings of cubic phase CoS₂, respectively (Fig. 1c). And the relevant diffraction peaks are labeled in the XRD pattern in Fig. 1e. The crystal structure of CoS₂ is shown in Fig. 1d. The nearest neighbor S atoms are covalently bonded to form a sulfur-sulfur (S-S) dimer. Divalent Co²⁺ cation is located in the center of an octahedron composed of six S₂²⁻ anions. Each sulfur is shared by three different octahedra and a single dimmer.³⁴ Fig. 1e gives the XRD patterns of CoS₂ NCs prepared at reaction time of 4h, 12h and 24h respectively. All the diffraction peaks observed here can be indexed to the pure cubic phase of CoS₂ with lattice constants: *a*=5.538 Å (JCPDS card No. 41-1471), indicating the highly purity of CoS₂ NCs with good crystallinity is synthesized through this modified MSS method. The corresponding lattice planes are further labeled in the pattern. And by this approach, no additional reagent is employed, avoiding the introduction of inevitable impurities, which is frequent by traditional MSS methods. Thus, no extra diffraction peaks, coming from flux or byproducts, are found in the pattern. The peaks observed become sharper gradually with the increasing reaction time. Based on the Debye-Scherrer equation, this evolution suggests the CoS₂ NCs becomes bigger with the increasing of reaction time.

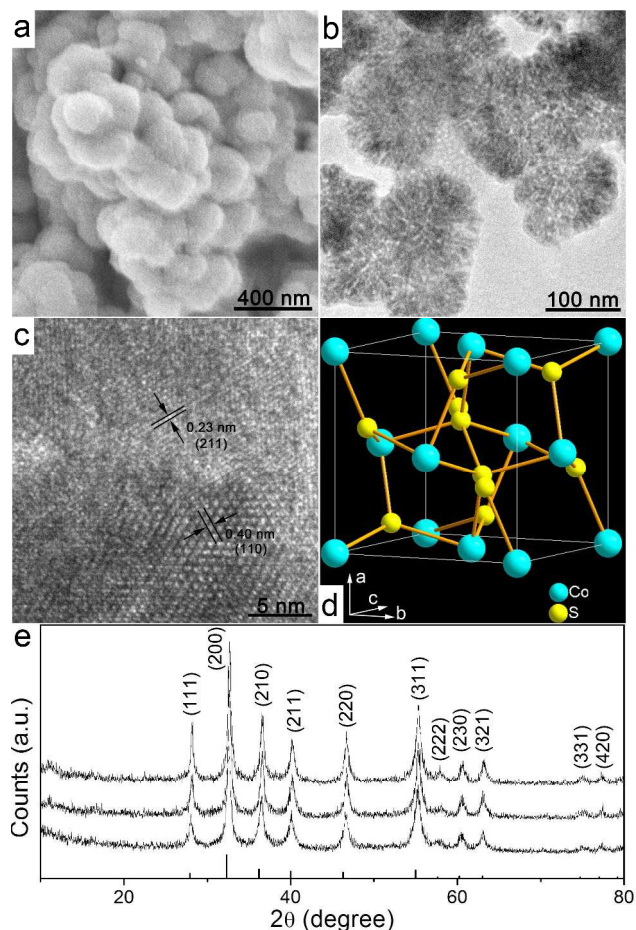


Figure 1. (a) SEM and (b) TEM (c) HRTEM images and (d) crystal structure of CoS₂ NCs synthesized at 180 °C for 4 h; XRD patterns of the CoS₂ prepared at 180 °C for 4 h (down), 12 h (middle), 24 h (up).

The chemical composition of the CoS₂ NCs was determined with an XPS measurement. Fig. 2 shows the XPS spectrum and EDX spectrum of as-synthesized products. The shake-up feature at higher binding energies can be assigned to Co²⁺ (Fig.2a).²³ A peak at 778.0 eV was found in the Co 2p spectrum, which can be attributed to Co-S bond (Fig.2b). The peak at 162.7 eV in the S 2p spectrum indicates the valence of -1. The peaks at 163.8 eV and 168.1 eV are ascribed to sulfur oxides.³⁵ All the peaks in Co 2p and S 2p spectra are consistent with the previous report.³⁶ From the EDX result, Co and S contents are of 33.1% and 66.9% respective, which corresponds to a Co/S ratio of 1:2, telling the final products of CoS₂.

To further confirm the structural information of CoS₂, a FTIR measurement is taken (Fig. S1). Thiourea and the final CoS₂ NCs are detected. Compared with the thiourea spectrum, CoS₂ NCs exhibits almost the same primary specific absorption peaks. The strong absorption peaks at 3333 and 3173 cm⁻¹, associated with the peaks at 1625 and 1507 cm⁻¹, were assigned to the vibration of N-H, and the peak at 616 cm⁻¹ is assigned to the vibration of -NH₂, peak at 1430 cm⁻¹ is assigned to C-N. Besides that, absorption peak at 2095 cm⁻¹ attributes to the vibration of -NCS, and the 1105 cm⁻¹ absorption peak is caused by the double bond between C and S. All these evidences above prove the fact that, the as-synthesized CoS₂ NCs are linked with the thiourea on surface of the porous structure by the means of Co-S-C-(NH₂)₂.

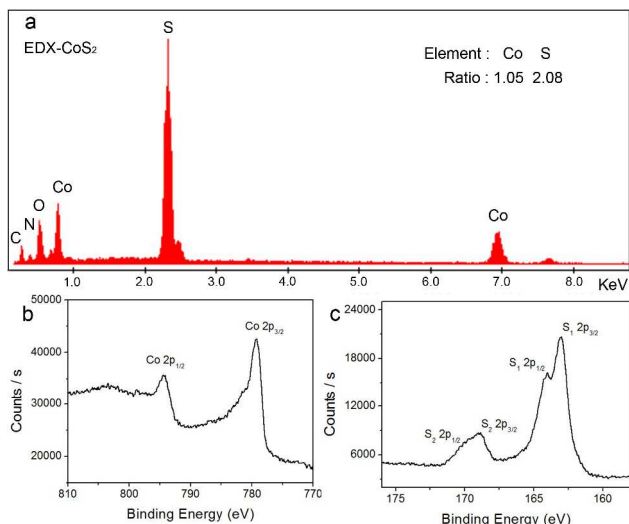


Figure 2. (a) EDX and (b and c) XPS spectrum of CoS₂ NCs synthesized at 180 °C for 4 h.

The thermal behavior of the as-synthesized CoS₂ was investigated by thermogravimetric analysis (TGA). There are three distinct regions of decline causing by weight loss (Fig. S2). The weight loss below 300 °C was mainly attributed to the water evaporation, which was adsorbed on the surface of sample. With the temperature going on to about 400 °C, the CoS₂ was decomposed into CoS, accompanied with the weight loss, and that above 600 °C was attributed to the thoroughly destruction of CoS₂ construction.^{37,38} The initial weight loss caused by thiourea decomposition goes the same with the earlier result of FTIR study, demonstrating the existence of thiourea on the surface of as-synthesized CoS₂ NCs.

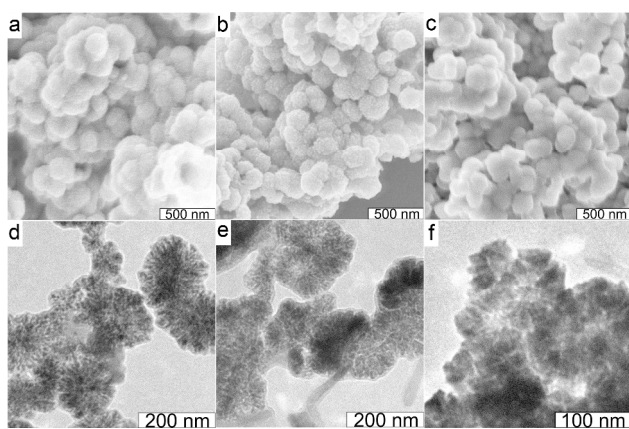


Figure 3. SEM and TEM images of CoS₂ prepared at 180 °C for (a, b) 4 h, (c, d) 12 h, (e, f) 24 h.

The morphology of as-synthesized CoS₂ NCs is characterized by SEM and TEM images, which are shown in Fig. 3. Samples are prepared by varying the reaction time from 4 h, 12 h to 24 h. As is described above, ~150 nm spheroidal CoS₂ NCs were formed when the reaction was preceded for 4 h (Fig. 3a). While, the ultra-small particles are clearly observed in the corresponding TEM image (Fig. 3d). It tells the fact that the sphere-like CoS₂ are composed by the aggregation of smaller ones, giving a result of porous surface structure. And the porous surface is significant to the later application of electrochemistry. This aggregation

growing process occurred during the initial stage. With the reaction time longer, about 12 h, size of particles increased to about 200 nm (Fig. 3b and e). The CoS₂ spheroids become smooth and angular when the reaction is maintained at 180 °C for 24 h, and the particle size increase to 250 nm (Fig. 3c and f). These results from the electron microscope are consistent to the conclusion from XRD analysis that the spheroidal CoS₂ NCs became bigger and more angular with the increase of reaction time.

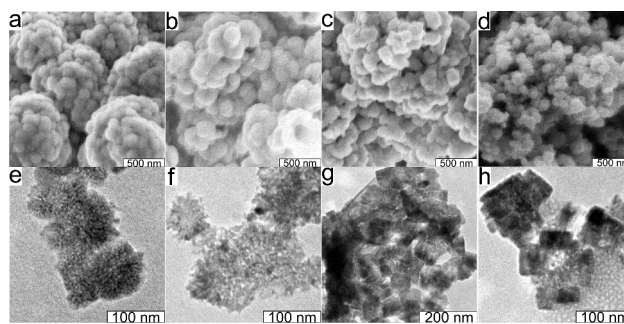


Figure 4. SEM and TEM images of the CoS₂ prepared at 180 °C for 4 h with different molar ratios of Co to S. (a, e) 1:3, (b, f) 1:5, (c, g) 1:7, (d, h) 1:10.

On the other hand, molar ratio of cobaltous nitrate to thiourea can also affect the morphology of the produced CoS₂ NCs. Fig. 4 reveals the SEM and TEM images of the CoS₂ NCs prepared at Co/S ratios of 1:3, 1:5, 1:7 and 1:10, respectively. It can be seen clearly from the SEM images that external morphology of CoS₂ NCs is gradually transitioned from spheroidal to angular with the increasing of Co/S ratio (Fig. 4 a-d). Higher Co/S ratio results in smaller NCs. The internal particle size is increased with the increase of Co/S ratio as shown in the TEM images (Fig. 4e-h). In addition, the internal particles gradually became square and angular. In all, both reaction time and the molar ratio of cobalt nitrate to thiourea can be employed to control the size and morphology of CoS₂ NCs.

3.2. Formation mechanism of the spherlike CoS₂ nanostructures

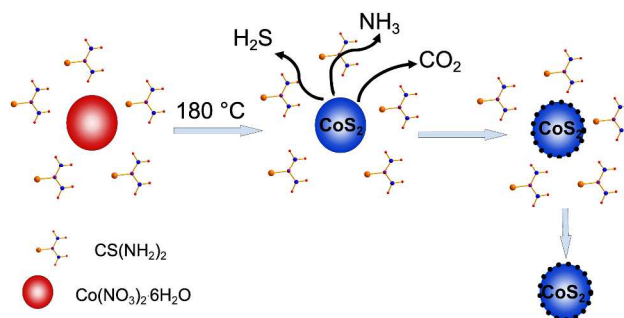


Figure 5. The formation process of the spherlike CoS₂ with porous surfaces nanostructures.

Based on size and morphological changes of the CoS₂ NCs and internal ultra-small nanoparticles with the increase of reaction time, a three-step synthesis mechanism is proposed as shown in Fig. 5. 1) The formation of spherlike CoS₂ at the early reaction stage. In this progress, the isomerism plays an important role. The isomerism of thiourea can offer an S-H bond, and the

neighbouring ones of isomerism can be further oxidized into S-S. And the resultant S_2^{2-} final reacted with Co^{2+} cation, forming the CoS_2 monomers.^{28,39} After the following growing stage, spheroidal CoS_2 NCs are produced; 2) the formation of porous structure on the CoS_2 NCs surface. As is known very well, the specific surface area is a key factor to the electrochemistry application. Thus, the surficial morphology is quite important to the as-synthesized CoS_2 NCs. Here in this approach, thiourea acts as the template. The excessive thiourea, which does not react with Co^{2+} cations, is then decomposed into H_2S , NH_3 and CO_2 under the high temperature surroundings.²⁶ These byproducts escape from CoS_2 NCs and result in a porous surface; 3) the aggregation of CoS_2 NCs. small CoS_2 NCs aggregate and become larger when the reaction is further proceeded. Meanwhile, the ultra-small particles inside of CoS_2 NCs also become larger and angular via Ostwald ripening mechanism. During this stage, the pores on the CoS_2 spheroid surface become smaller and disappear eventually. The surface of CoS_2 particles becomes smooth.

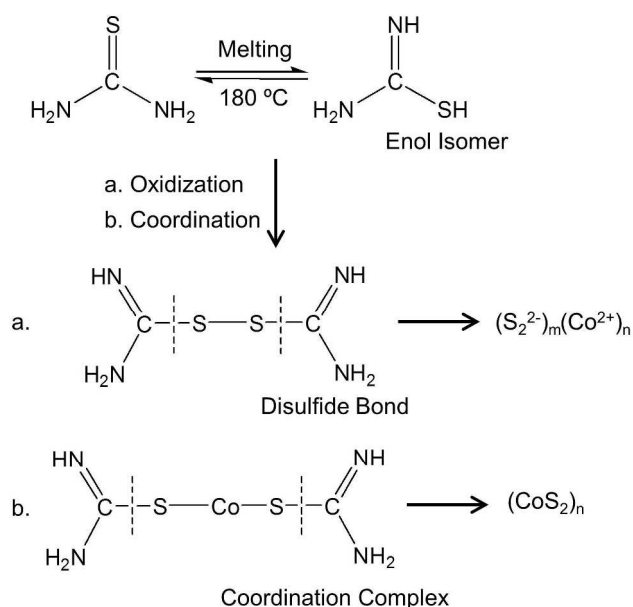


Figure 6. The formation mechanism of the spherulike CoS_2 with porous surfaces nanostructures.

In this synthesis pathway, thiourea plays three roles. First, it provides a uniform environment for the growth of CoS_2 as a flux, resulting a relatively low reaction temperature, 180 °C. Secondly, the isomerism of thiourea offers the S_2^{2-} for final formation of CoS_2 as a reactant. As is shown in Fig. 6, the thiourea converts into S_2^{2-} with two major approaches. When heated with 180 °C, to the fusion state, the thiourea could transform with its isomeride, enolisomer, freely. The isomer would oxidize into a disulfide compound firstly, then coordinate with Co cations with the formation of $(S_2^{2-})_m(Co^{2+})_n$. On the other hand, the isomer prefers to coordinate with Co cations, forming the complex of Co-thiourea. And then decompose into $(CoS_2)_n$. With the act of thiourea, both the oxidization and coordination approach can achieve the final CoS_2 NCs. Finally, it decomposes into gases at high temperature as a structure-directing agent, leading to the porous structure on CoS_2 spheroid surface.

3.3. Electrochemical performances of CoS_2 NCs

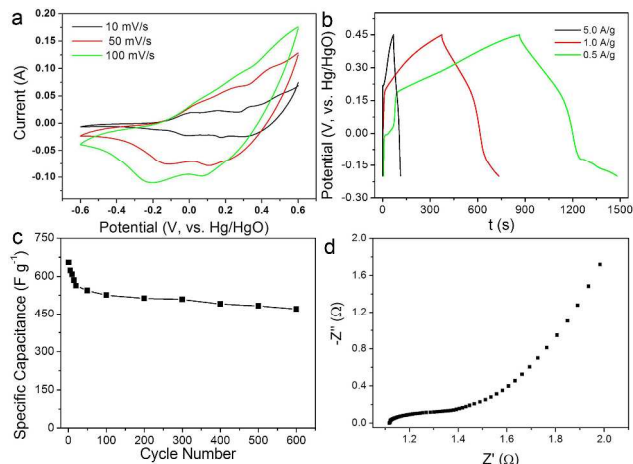
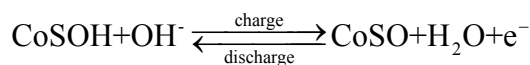
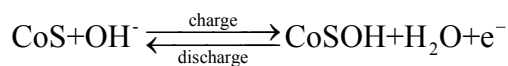


Figure 7. (a) CV curves of electrodes fabricated from CoS_2 (electrolyte: 2 M KOH) at various scan rates: 5, 10, and 50 $mV\ s^{-1}$; (b) Charge-discharge behavior of a CoS_2 electrode at different current density of 0.5, 1, and 5 $A\ g^{-1}$; (c) Cycling performance at a current density of 0.5 $A\ g^{-1}$; (d) Nyquist plots at the range of 0.1 Hz-100 KHz.

The cyclic voltammetry (CV) curves were recorded on a CoS_2 electrode in 2M KOH solution at sweep rates of 10, 50 and 100 mV/s , in a potential range from -0.6 to 0.6 V (Fig. 7a). The specific procedure for electrode is shown in Supporting Information. An Hg/HgO electrode was used as a reference electrode, Pt electrode was employed as a counter electrode. The CV curve shape of CoS_2 electrode is different from the regular rectangular CV curve of an electric double-layer electrode,⁴⁰ suggesting the different capacitance characteristics of the CoS_2 electrode. Two typical redox peaks were observed in the CV curves of the CoS_2 electrode, indicating that the capacity of the CoS_2 electrode mainly results from the pseudocapacitive capacitance. The O1 peak at ~ 0.15 V is attributed to the conversion of Co (II) into Co (III). The O2 peak at 0.35 V is assigned to the conversion of Co (III) into Co (IV). The corresponding R1 and R2 peaks show the similar situation to the oxidation process, suggesting that the redox reactions on CoS_2 electrode in the alkaline solution are electrochemical reversible. This feature of the CoS_2 electrode results in a much higher electric capacity than that of the conventional double-layer capacitors. The redox reactions that occur at the interface between CoS_2 electrode and the alkaline solution are as the follows.⁹



The charge-discharge behaviors of the CoS_2 electrode in potential range between -0.2 and 0.45 V at different current densities are shown in Fig. 7b. The non-linear variation of the potential versus time further illustrates a typical pseudocapacitive performance resulting from the electrochemical redox reactions occurred at the CoS_2 electrode/electrolyte interface. The specific capacitance was calculated using the following equation of $C = I \Delta t / (m \Delta V)$, where C ($F\ g^{-1}$) is the specific capacitance; I (mA) is the discharge

current; Δt (s) is the discharge time; ΔV (V) is the potential change during discharge; and m (mg) is the mass of active material.²⁸ The specific capacitances of the CoS₂ electrode are 654, 595 and 499 F g⁻¹ at discharge current densities of 0.5, 1 and 5 A g⁻¹ respectively. The higher pseudocapacitance at low current density can be explained that the electrolyte ions have sufficient time to enter and diffuse into the porous structure of the CoS₂ electrode at lower current densities.²⁴ A negligible dissymmetry is observed in the charge-discharge curves, it may be caused by the non-completely reversible redox reaction during the electrochemistry process. Fig. 7c shows the charge-discharge cycles at a current density of 0.5 A g⁻¹ in 6 M KOH electrolyte solution. The as-synthesized products can still retain 72% of capacitance value after 600 cycles, about 470 F g⁻¹. The electrochemical behaviors of the CoS₂ electrode were further explored by electrochemical impedance measurements. Its Nyquist plot consists of a semicircle in the high frequency region and a linear slop in the low frequency region (Fig. 7d). The linear slope in the low frequency region suggests that the charge-transfer resistance might result from the electrical conductivity of CoS₂ NCs.⁴¹ The charge-transfer resistance was calculated from the Nyquist plot as 1.3 Ω , suggesting that CoS₂ is a suitable active electrode material for supercapacitor.

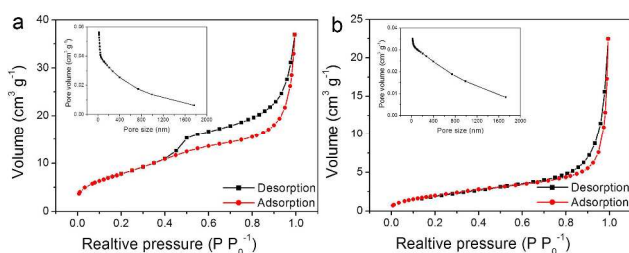


Figure 8. N₂ adsorption-desorption isotherms and pore size distribution (inset) of the CoS₂ prepared at (a) 4 h and (b) 24 h;

Nitrogen adsorption-desorption isotherms of two CoS₂ NCs samples, which are prepared at reaction time of 4h and 24 h, are shown in Fig. 8a and 8b, respectively. The insets are the corresponding Barrett-Joyner-Halenda (BJH) pore volumes obtained from the branches of the isotherm. The BET specific surface areas of these two CoS₂ NCs samples are 29.30 and 7.89 m²g⁻¹, respectively. The larger BET area of CoS₂ NCs sample prepared at shorter reaction time is attributed to their smaller size and porous surface. The charge-discharge behaviors of the CoS₂ electrode synthesized at reaction time of 4 h and 24 h are shown in Fig. S3. The specific capacitances of the two CoS₂ electrodes are 654 and 385 F g⁻¹, respectively. The higher capacitance the CoS₂ NCs synthesized with 4 h reaction time is largely attributed to its larger specific surface area and porous surface that provides good accessibility for the electrolyte ions. Similar CV curves at different sweep rates were obtained on the CoS₂ electrode synthesized at 24 h reaction time (Fig. S4).

Conclusion

In summary, spherelike CoS₂ NCs with porous surfaces were successfully prepared by a modified MSS method. In this synthesis pathway, thiourea acts as both sulfur source and flux wherein it decreases the reaction temperature and leads to milder reaction conditions. This MSS pathway could also be used in the

synthesis of other sulfides. The increase of reaction time causes an increase in the size of CoS₂ NCs and a decrease in the specific area. The increase in feed Co/S ratio from 1:3 to 1:10 also shows similar effects. The specific capacitance of the electrodes fabricated with CoS₂ NCs reached 654 F g⁻¹. These results indicate that this modified MSS method can be used for the large-scale growth of metal sulfide nanostructure and CoS₂ NCs is a potential electrode material for supercapacitors.

Acknowledgment

This work was supported by the National Sciences Foundation of China (No.21271082, 21301066 and 21371068)

Notes and references

- State Key Laboratory of Inorganic Synthesis and Preparative Chemistry, College of Chemistry, Jilin University, 2699 Qianjin Street, Changchun 130012, P. R. China. Fax: (+86) 431-85168316; Tel: (+86) 431-85168316; E-mail: liuxy@jlu.edu.cn
- † Electronic Supplementary Information (ESI) available: [details of any supplementary information available should be included here]. See DOI: 10.1039/b000000x/
- X. W. Yang, C. Cheng, Y. F. Wang, L. Qiu and D. Li, *Science*, 2013, **341**, 534.
 - T. Kuila, A. K. Mishra, P. Khanra, N. H. Kim and J. H. Lee, *Nanoscale*, 2013, **5**, 52.
 - S. Fiorenti, J. Guanetti, Y. Guezennec and S. Onori, *J. Power Sources*, 2013, **241**, 112.
 - L. Yu, G. Q. Zhang, C. Z. Yuan and X. W. Lou, *Chem. Commun.*, 2013, **49**, 137.
 - A. L. M. Reddy, M. M. Shaijumon, S. R. Gowda and P. M. Ajayan, *J. Phys. Chem. C*, 2010, **114**, 658.
 - W. Du, R. M. Liu, Y. W. Jiang, Q. Y. Lu, Y. Z. Fan and F. Gao, *J. Power Sources*, 2013, **227**, 101.
 - F. Jiao, A. H. Hill, A. Harrison, A. Berko, A. V. Chadwick and P. G. Bruce, *J. Am. Chem. Soc.*, 2008, **130**, 5262.
 - D. W. Wang, F. Li and H. M. Cheng, *J. Power Sources*, 2008, **185**, 1563.
 - X. T. Luo, X. F. Li, H. Zhang and B. Yang, *Part. Part. Syst. Charact.*, 2013, **30**, 501.
 - T. Zhu, J. S. Chen and X. W. Lou, *J. Mater. Chem.*, 2010, **20**, 7015.
 - H. Jiang, J. Ma and C. Z. Li, *Chem. Commun.*, 2012, **48**, 4465.
 - N. Fechler, G. A. Tiruye, R. Marcilla and M. Antonietti, *RSC Adv.*, 2014, **4**, 26981.
 - C. Z. Yuan, X. G. Zhang, L. H. Su, B. Gao and L. F. Shen, *J. Mater. Chem.*, 2009, **19**, 5772.
 - X. J. Zhang, W. H. Shi, J. X. Zhu, W. Y. Zhao, J. Ma, S. Mhaisalkar, T. L. Maria, Y. H. Yang, H. Zhang, H. H. Hng and Q. Y. Yan, *Nano Res.*, 2010, **3**, 643.
 - L. Zhang, H. B. Wu and X. W. Lou, *Chem. Commun.*, 2012, **48**, 6912.
 - S. M. Liu, J. X. Wang, J. W. Wang, F. F. Zhang, F. Liang and L. M. Wang, *CrystEngComm*, 2014, **16**, 814.
 - Y. J. Sun, C. Liu, D. C. Grauer, J. K. Yano, J. R. Long, P. D. Yang and C. J. Chang, *J. Am. Chem. Soc.*, 2013, **135**, 17699.
 - G. C. Huang, T. Chen, Z. Wang, K. Chang and W. X. Chen, *J. Power Sources*, 2013, **235**, 122.
 - J. Pu, Z. H. Wang, K. L. Wu, N. Yu and E. H. Sheng, *Phys. Chem. Chem. Phys.*, 2014, **16**, 785.
 - Z. S. Yang, C. Y. Chen and H. T. Chang, *J. Power Sources*, 2011, **196**, 7874.
 - S. Y. Chae, Y. J. Hwang, J. H. Choi and O. S. Joo, *Electrochimica Acta.*, 2013, **114**, 745.
 - Q. H. Wang, L. F. Jiao, H. M. Du, J. Q. Yang, Q. N. Huan, W. X. Peng, Y. C. Si, Y. J. Wang and H. T. Yuan, *CrystEngComm*, 2011, **13**, 6960.
 - J. Y. Lin and S. W. Chou, *RSC Adv.*, 2013, **3**, 2043.

- 24 H. Z. Wan, X. Ji, J. J. Jiang, J. W. Yu, L. Mao, L. Zhang, S. W. Bie, H. C. Chen and Y. J. Ruan, *J. Power Sources*, 2013, **243**, 396.
- 25 Y. D. Yin, C. K. Erdonmez, A. Cabot, S. Hughes and A. P. Alivisatos, *Adv. Funct. Mater.*, 2006, **16**, 1389.
- 5 26 W. J. Dong, X. B. Wang, B. J. Li, L. N. Wang, B. Y. Chen, C. R. Li, X. Li, T. R. Zhang and Z. Shi, *Dalton Trans.*, 2011, **40**, 243.
- 27 S. J. Bao, C. M. Li, C. X. Guo and Y. Qiao, *J. Power Sources*, 2008, **180**, 676.
- 28 B. Wang, J. Park, D. W. Su, C. Y. Wang, H. Ahn and G. X. Wang, *J. Mater. Chem.*, 2012, **22**, 15750.
- 10 29 Y. Hayashi, T. Kimura and T. Yamaguchi, *J. Mater. Sci.*, 1986, **21**, 2876.
- 30 W. Z. Wang, B. Q. Zeng, J. Yang, B. Poudel, J. Y. Huang, M. J. Naughton and Z. F. Ren, *Adv. Mater.*, 2006, **18**, 3275.
- 15 31 X. Zhang, P. P. Yang, C. X. Li, D. Wang, J. Xu, S. L. Gai and J. Lin, *Chem. Commun.*, 2011, **47**, 12143.
- 32 Z. Y. Cai, X. R. Xing, R. B. Yu, X. Y. Sun and G. R. Liu, *Inorg. Chem.*, 2007, **46**, 7423.
- 33 Y. Tian, D. R. Chen, X. L. Jiao and Y. Z. Duan, *Chem. Commun.*, 2007, **20**, 2072.
- 20 34 P. J. Brown, K. U. Neumann, A. Simon, F. Ueno and K. R. A. Ziebeck, *J. Phys.: Condens. Matter.*, 2005, **17**, 1583.
- 35 A. Galtayries, C. Cousi, S. Zanna and P. Marcus, *Surf. Interface Anal.*, 2004, **36**, 997.
- 25 36 C. Zhao, D. Q. Li and Y. J. Feng, *J. Mater. Chem. A*, 2013, **1**, 5741.
- 37 A. N. Grace, R. Ramachandran, M. Vinoba, S. Y. Choi, D. H. Chu, Y. Yoon, S. C. Nam and S. K. Jeong, *Electroanalysis*, 2014, **26**, 199.
- 38 B. H. Qu, Y. J. Chen, M. Zhang, L. L. Hu, D. N. Lei, B. A. Lu, Q. H. Li, Y. G. Wang, L. B. Chen and T. H. Wang, *Nanoscale*, 2012, **4**, 7810.
- 30 39 S. Wang, Q. Y. Gao, J. C. Wang, *J. Phys. Chem. B*, 2005, **109**, 17281.
- 40 S. J. Peng, L. L. Li, H. T. Tan, R. Cai, W. H. Shi, C. C. Li, S. G. Mhaisalkar, M. Srinivaan, S. Ramakrishna and Q. Y. Yan, *Adv. Funct. Mater.*, 2014, **24**, 2155.
- 35 41 S. M. Paek, E. Yoo and I. Honma, *Nano Lett.*, 2009, **9**, 72